GLOBAL ENGINEERS & TECHNOLOGISTS REVIEW
www.getview.org

ANALYSIS OF THE HIGH TEMPERATURE SUPERCONDUCTING MAGNETIC PENETRATION DEPTH USING THE BLOCH NMR EQUATIONS

UNO E UNO[1] and MOSES E EMETERE[2]

[1, 2] Department of Physics
Federal University of Technology Minna
P.M.B 65, Minna, NIGERIA
[1]emetere@yahoo.com

ABSTRACT

The Bloch-NMR diagnostic tool has shown good efficiency not only analyzing biological and physiological properties of living tissues. The Bloch-NMR has been used in this research work to analyze the penetration depths of superconducting material and thin film. From the two well known London penetration depths, various relationships between the penetration depth and other superconducting quantities were derived (which are theoretically and experimentally valid). The major objective is to explore new ways penetration depths can be measured. A new superconducting quantity (penetration velocity) was discussed - whose relationship with other superconducting quantities were worked out for further research

Keywords: *Bloch Equation, Magnetic Penetration Depth, Superconductivity, Moun-spin, Penetration Velocity.*

1.0 INTRODUCTION

Many tunnelling measurements of electron doped cuprates and other HTS samples support the s-wave picture while other STM data supports the d-wave pairing (Ruslan *et al*., 2000) & (Gordon *et al*., 2008). The London penetration depth to a large extent has given a precise measure of the quasiparticle population though it has been reported that at low temperatures, there is an exponential suppression of quasiparticle as stated by Fumiaki *et al*. (1998), (which supports the s-wave pairing). One of the unique properties of the cuprates is its ability to allow magnetic flux to thread them by means of vortices of flux. Each vortex is the normal region in the sample, while the regions in between vortices are the superconducting part of the material. Lately, interest has shifted to how externally applied magnetic fields penetrate the cuprates and how wide a single vortex might be in such cases. Significantly, the penetration depth has been experimentally proven to be proportional to the volume of the magnetic field penetrating the samples from different sides i.e. along and perpendicular to the c-axis. Gordon *et al*. (2008) in his research shows when the excitation field is applied parallel to the c-axis, only the in-plane currents penetrates and λ_{ab} is measured directly. When the excitation field is applied perpendicular to the c-axis, currents circulates in both the ab - plane and along the c-axis direction. The Bloch NMR equation has successfully used to study biological and physiological properties of living tissue as discussed by Awojoyogbe (2004) & (2003). Besides medical applications, the Bloch NMR equation can be used to investigate the thermodynamic properties of system. One of the Bloch NMR successes is the Wegner distribution function (Wigner, 1932), (which is to provide a framework for the treatment of quantum-mechanical problems), Kirkwood distribution function (Kirkwood, 1993) and the phase-space correspondence of the Bloch equations (O'Connell, 1985). Through the re-modeled Bloch-NMR equations, another parameter for measuring penetration depth was theoretically discovered.

2.0 METHODS

2.1 Theoretical Remodelling Bloch-NMR Equation

In this study, a mathematical algorithm to describe in detail the translational mechanical properties of the Bloch NMR equation was developed. A sample of HTS sample can be analyzed by the x, y, z component (in the rotating frame) of magnetization given by the Bloch equations which may be written as follows:

$$\frac{dM_x}{dt} = \Delta\omega M_y - \frac{M_x}{T_2} \quad (1)$$

$$\frac{dM_y}{dt} = -\Delta\omega M_x - \omega_1 M_z - \frac{M_y}{T_2} \quad (2)$$

$$\frac{dM_z}{dt} = -\omega_1 M_y - \frac{(M_z - M_0)}{T_1} \quad (3)$$

Where $\Delta\omega = \omega_1 - \omega_0$ the frequency difference between Larmor frequency and frame of reference, $\omega_1 = -\gamma B_1$ is the Rabi frequency, $\omega_0 = -\gamma B_0$ is the Larmor frequency, M_x, M_y are the transverse magnetization, M_z is the longitudinal magnetization, M_o is the equilibrium magnetization.

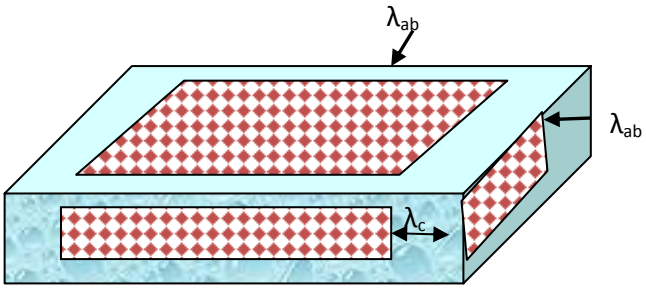

Figure 1: A HTS sample under consideration

Figure 1 shows a HTS sample with thickness 2c, width 2b, and length 2a. It has two different London penetration depths λ_{ab} and λ_c. A magnetic field is applied in the z-direction so demagnetizing corrections are absent. To facilitate comparism with the copper oxides, the y-direction is along the c-axis and x and z directions correspond to the a and b axes. So $\lambda_{xx,yy} = \lambda_{ab}$ and $\lambda_{yy} = \lambda_c$.The in-plane supercurrent flowing in the x-direction penetrates from the top and bottom faces a distance λ_{ab}. Interplane(c-axis) supercurrent flowing in the y-direction penetrates from the left and right edges a distance λ_c. This assumption transforms the bloch as follows:

$$\frac{dM_x}{d\lambda_{ab}}\frac{d\lambda_{ab}}{dt} = \frac{dM_x}{dt} \quad (4)$$

$$\frac{dM_y}{d\lambda_c}\frac{d\lambda_c}{dt} = \frac{dM_y}{dt} \quad (5)$$

$$\frac{dM_z}{d\lambda_{ab}}\frac{d\lambda_{ab}}{dt} = \frac{dM_z}{dt} \quad (6)$$

$$\frac{dM_x}{d\lambda_{ab}} = \frac{\Delta\omega}{v_{ab}}M_y - \frac{M_x}{v_{ab}T_2} \quad (7)$$

$$\frac{dM_y}{d\lambda_c} = \frac{-\Delta\omega M_x}{v_{ab}} + \frac{\omega_1 M_z}{v_{ab}} - \frac{M_y}{v_c T_2} \quad (8)$$

$$\frac{dM_z}{d\lambda_{ab}} = \frac{-\omega_1 M_y}{v_{ab}} - \frac{(M_z - M_0)}{v_{ab}T_1} \quad (9)$$

Where; $v_{ab} = \frac{d\lambda_{ab}}{dt}$, $v_c = \frac{d\lambda_c}{dt}$

The solution of the above equations can be arranged in matrix form as shown below

$$\begin{bmatrix} -v_c & \Delta\omega T_2 v_{ab} & 0 \\ -\Delta\omega v_c T_2 & v_c & T_2\omega_1 v_{ab} \\ 0 & -v_{ab}T_1\omega_1 & -v_c \end{bmatrix}\begin{bmatrix} M_x \\ M_y \\ M_z \end{bmatrix} = \begin{bmatrix} 0 \\ 0 \\ v_c M_o \end{bmatrix} \quad (10)$$

The matrix multiplication as shown below leads to the steady solutions of the Bloch equations in the rotating frame of reference are shown below.

$$M_x = \frac{\omega_1 \Delta\omega v_c v_{ab}^2 T_2^2 M_0}{-v_{ab}^2 - \omega_1^2 v_{ab} v_c T_1 T_2 - \Delta\omega^2 v_{ab} v_c^2 T_2^2} \quad (11)$$

$$M_y = \frac{T_2\omega_1 v_{ab} v_c M_0}{-v_{ab}^2 - \omega_1^2 v_{ab} v_c T_1 T_2 - \Delta\omega^2 v_{ab} v_c^2 T_2^2} \quad (12)$$

$$M_z = \frac{-\nu_{ab}^2 + \Delta\omega^2 \nu_{ab}\nu_c^2 T_2^2 M_0}{-\nu_{ab}^2 - \omega_1^2 \nu_{ab}\nu_c T_1 T_2 - \Delta\omega^2 \nu_{ab}\nu_c^2 T_2^2} \quad (13)$$

These solutions directly give the frequency response of the magnetization. This idea gives the possibilities of quantitatively calculating the measured signal if a spin system is characterized by relaxation times T_1 and T_2. The term $\omega_1^2 \nu_{ab}\nu_c T_1 T_2$ is proportional to the radio frequency power P. At the state of no saturation i.e. for low power P, this term ($\omega_1^2 \nu_{ab}\nu_c T_1 T_2$) is small $\omega_1^2 \nu_{ab}\nu_c T_1 T_2 \ll 1$

$$M_x = \frac{\omega_1 \Delta\omega \nu_c \nu_{ab}^2 T_2^2 M_0}{-\nu_{ab}^2 - \Delta\omega^2 \nu_{ab}\nu_c^2 T_2^2} \quad (14)$$

$$M_y = \frac{T_2 \omega_1 \nu_{ab}\nu_c M_0}{-\nu_{ab}^2 - \Delta\omega^2 \nu_{ab}\nu_c^2 T_2^2} \quad (15)$$

M_x is in phase with the exciting alternating field B_1 and M_y is 90° out of phase with the exciting alternating field B_1.

$$M_x \approx (\omega_1 M_0) \frac{\Delta\omega \nu_c \nu_{ab}^2 T_2^2}{-\nu_{ab}^2 - \Delta\omega^2 \nu_{ab}\nu_c^2 T_2^2} = \omega_1 M_0 F(\Delta\omega) \quad (16)$$

$$M_y \approx (\omega_1 M_0) \frac{T_2 \nu_{ab}\nu_c}{-\nu_{ab}^2 - \Delta\omega^2 \nu_{ab}\nu_c^2 T_2^2} = \omega_1 M_0 G(\Delta\omega) \quad (17)$$

ν_{ab} and ν_c are the penetration velocity along the 'ab' and 'c' axes respectively. F(Δω) and G(Δω) are the dispersion and the absorption for a particular kind of line known as the Lorentzian line. Before the superconducting state is attained, the magnetic flux is written as

$$M_{tot} = M_{ext} - M_{HTS} \quad (18)$$

When the HTS sample starts superconducting, the magnetic flux expels-leaving the net magnetic flux as

$$M_{tot} = - M_{HTS} \quad (19)$$

Experimentally, $M_{HTS} \cong \frac{M_0}{4\pi\left(\frac{\lambda}{\xi}\right)^2} In\left(\frac{\lambda}{\xi}\right)$

λ and ξ are the penetration depth and the vortex cross section in the HTS material. Here the total magnet flux is the transverse magnetic flux along the y-axis i.e. $M_y = M_{tot}$

Therefore, $M_y = - \frac{M_0}{4\pi\left(\frac{\lambda}{\xi}\right)^2} In\left(\frac{\lambda}{\xi}\right)$

$$\frac{T_2 \omega_1 \nu_{ab}\nu_c M_0}{-\nu_{ab}^2 - \Delta\omega^2 \nu_{ab}\nu_c^2 T_2^2} = - \frac{M_0}{4\pi\left(\frac{\lambda}{\xi}\right)^2} In\left(\frac{\lambda}{\xi}\right) \quad (20)$$

$$4\pi \left(\frac{\lambda_{ab}}{\xi_{ab}}\right)^2 T_2 \omega_1 \nu_{ab}\nu_c M_0 = In\left(\frac{\lambda_{ab}}{\xi_{ab}}\right)(\nu_c^2 + \Delta\omega^2 \nu_{ab}\nu_c^2 T_2^2) \quad (21)$$

Equation (21) can be written into two forms according to the terms ν_{ab} and ν_c.

$$4\pi \left(\frac{\lambda_{ab}}{\xi_{ab}}\right)^2 \omega_1 = In\left(\frac{\lambda_{ab}}{\xi_{ab}}\right) \Delta\omega^2 T_2 \quad (22)$$

Where $\frac{\lambda_{ab}}{\xi_{ab}} = \frac{\lambda_{ab}(0)}{\xi_{ab}(0)} \sqrt{\frac{\left(1 - \frac{T}{T_c}\right)}{\left(1 - \left(\frac{T}{T_c}\right)^4\right)}}$

$\frac{T}{T_c}$ is the reduced temperature

$$\lambda_{ab} = \xi_{ab} \exp\left(\frac{4\pi \left(\frac{\lambda_{ab}(0)}{\xi_{ab}(0)}\right)^2 \frac{\left(1-\frac{T}{T_c}\right)^{\frac{1}{2}}}{\left(1-\left(\frac{T}{T_c}\right)^4\right)^{\frac{1}{2}}} \omega_1}{2\omega^2 \tau_2} \right) \quad (23)$$

This shows directly proportional relationship between penetration depth and coherent depth with a constant i.e.

$$\exp\left(\frac{4\pi \left(\frac{\lambda_{ab}(0)}{\xi_{ab}(0)}\right)^2 \frac{\left(1-\frac{T}{T_c}\right)^{\frac{1}{2}}}{\left(1-\left(\frac{T}{T_c}\right)^4\right)^{\frac{1}{2}}} \omega_1}{2\omega^2 \tau_2} \right)$$

. Figure 2 (a) is an illustrational graph of λ_{ab} and $\frac{T}{T_c}$ when ξ_{ab} = 80nm.

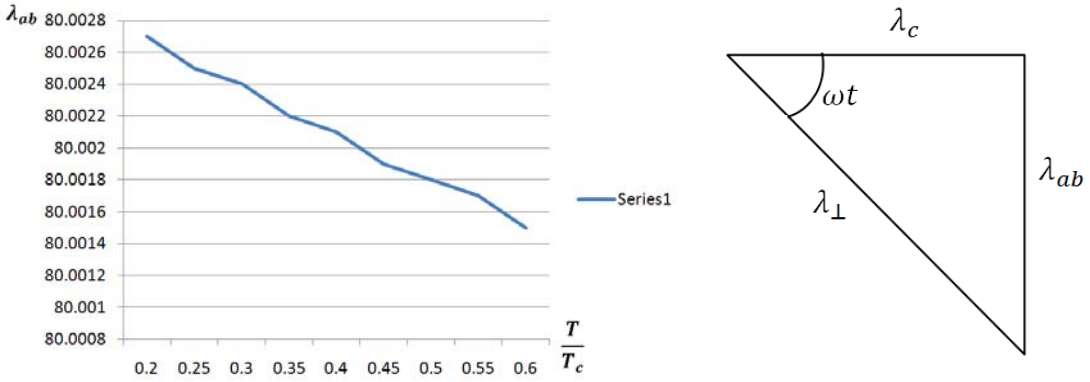

(a) **(b)**

Figure 2: (a) Illustrational graph of λ_{ab} and $\frac{T}{T_c}$ when ξ_{ab} = 80nm. **(b)** the triangle defining the phase angle of the two penetration depths

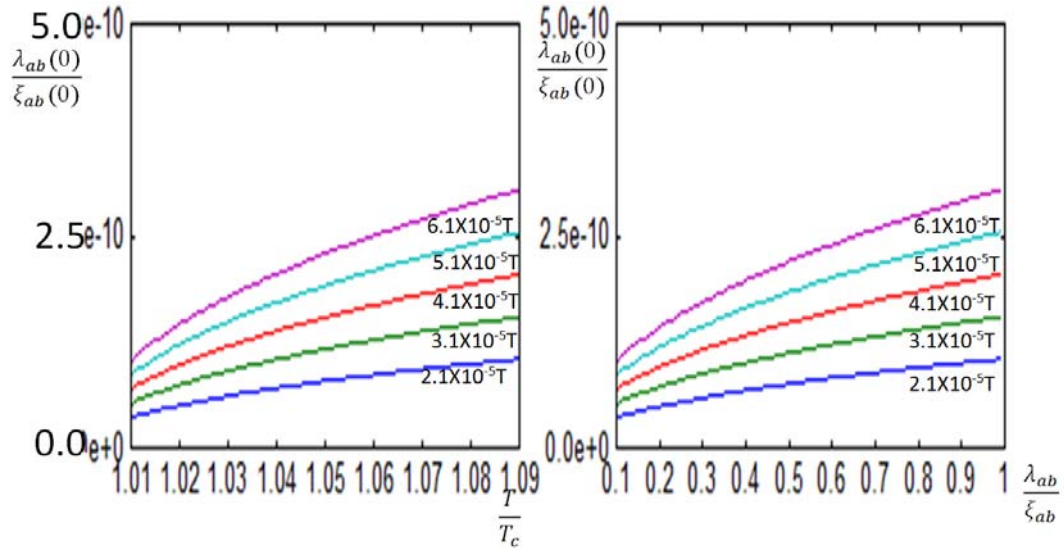

Figure 3: The relationship between ground state penetration depth with the reduced temperature and the magnetic penetration depth. Five lines showing the increasing external magnetic field.

The second form of equation (22) is given below

$$4\pi\left(\frac{\lambda_c}{\xi_c}\right)^2 T_2\,\omega_1 v_0 = \ln\left(\frac{\lambda_c}{\xi_c}\right)\left(v_0^2 - \Delta\omega^2 v_0^2 T_2^2\right) \tag{24}$$

Considering motion of the transverse magnetization when $\omega_1 = \gamma B_1(t) = \cos\omega t$ equation transforms to

$$a\frac{d^2\lambda_c}{dt^2} \quad b\frac{d\lambda_c}{dt} = c\cos\omega t \tag{25}$$

Where $a = \ln\left(\frac{\lambda_c}{\xi_c}\right)$, $b = \ln\left(\frac{\lambda_c}{\xi_c}\right)\Delta\omega^2 T_2^2$, $c = 4\pi\left(\frac{\lambda_c}{\xi_c}\right)^2 T_2$

$\lambda_\perp$ is the effective penetration depth. From Figure 2 (b) the solution of the two penetration depths are:

$$\left.\begin{aligned}\lambda_{ab} &= \lambda_\perp \sin(\omega_o t)\\ \lambda_c &= \lambda_\perp \sin(\omega_o t)\end{aligned}\right\} \tag{26}$$

From which two values for $\lambda_\perp$ was obtained i.e

$$\lambda_\perp = -\frac{4\pi\left(\frac{\lambda_c}{\xi_c}\right)^2 T_2}{\ln\left(\frac{\lambda_c}{\xi_c}\right)\omega_o}$$

and $\lambda_\perp = 0$

Therefore the penetration depth along the c-axis is given as

$$\lambda_c = -\frac{4\pi\left(\left(\frac{\lambda_c(0)}{\xi_c(0)}\right)^2\frac{\left(1-\frac{T}{T_c}\right)}{\left(1-\left(\frac{T}{T_c}\right)^4\right)}\right)T_2}{\ln\left(\left(\frac{\lambda_c(0)}{\xi_c(0)}\right)^2\frac{\left(1-\frac{T}{T_c}\right)}{\left(1-\left(\frac{T}{T_c}\right)^4\right)}\right)\omega_o}\cos(\omega_o t) \tag{27}$$

The minus sign shows the direction of the motion of the transverse magnetization or the reversible magnetization effects.

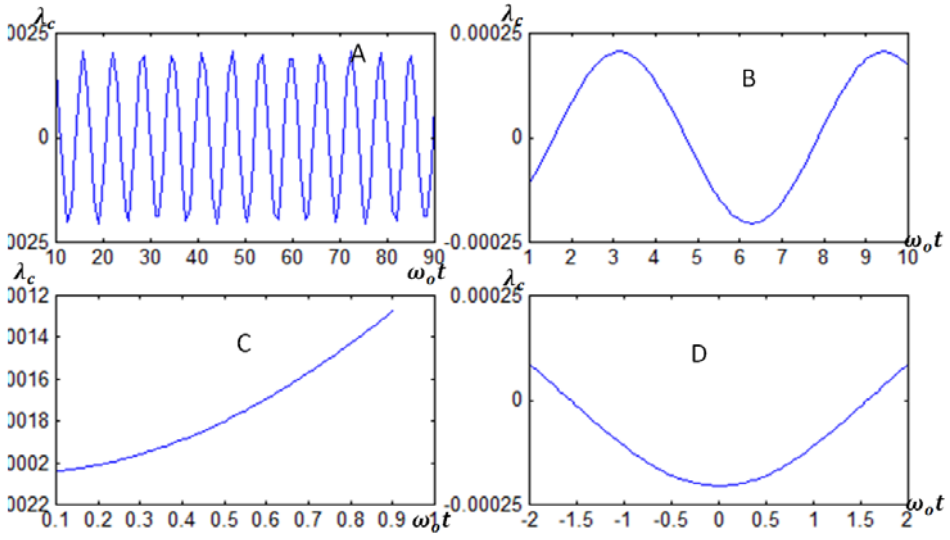

Figure 4 : Analysis of penetration depth (λ_c) with respect to varying phase angles ($\omega_o t$) when $\frac{\lambda_c(0)}{\xi_c(0)} = \frac{T}{T_c}$ provided $\frac{T}{T_c} \gg 1$

Figure 2(a), Figure 3 and Figure 4, expresses the two critical fields i.e. H_{c1} and H_{c2} respectively. The superconducting material reaches the Meissner state under the critical field H_{c1}. When the field exceeds H_{c1}, the Abrikosov or mixed state is reached. Beyond the mixed state is the maximum critical field value H_{c2}.At any critical field values H_{c1} and H_{c2}, these material exhibit a mixed behavior that allow magnetic flux to penetrate them by means of vortices of flux (as shown in figure 3 where varying magnetic fields between $2.1X10^{-5}T$ and $6.1X10^{-5}T$ were made to penetrate the system). The regions in between vortices are the superconducting part of this material. Each vortex in particular carries one fluxoid ϕ_o (the fundamental unit of quantized flux).

2.2 Application of Our Study to the Muon-Spin Relaxation Rate

The transverse field muon spin relaxation (TF-MSR) has good similarities with the present study in that

(i) It is operated at low magnetic fields for $H_{ext} \leq 0.3T$.
(ii) Each muon precess in its local magnetic field B_1 with the Larmor frequency $\omega_1 = \gamma B_1$
(iii) The function of the spin polarization function $P_\mu(t)$ is similar to the Lorentzian function $F(\Delta\omega)$ because they are both oscillatory in characteristics.
(iv) The magnetic moment is directly related to the magnetic penetration depth.

Past research work has shown that the c-axis oriented thin films (Pattanaik and Mudur, 1993) had given a sizeable anisotropy of the superconducting properties with anisotropy ratios (λ_c / λ_{ac}) ranging from about 1.6 to about 2.5. This gives equation (8) preference under this section. The motive is to inquire the relationship between the ratios of the penetrating velocities (λ_c / λ_{ab}) to other known quantities. Using the Fourier transform $P(t) = \frac{1}{2\pi}\int_{-\infty}^{\infty} F(\Delta\omega)e^{-i\Delta\omega t}\,dt$ coupled to dynamic Kubo-Toyabe function (which expresses the spin polarization) of the form (Hayano *et al*., 1979).

$$P(t) = P_z(t)\exp\left(-\frac{t}{\tau_o}\right) + \frac{1}{\tau_o}\int_0^t P_z(t')\exp\left(-\frac{t'}{\tau_o}\right).P_z(t-t')dt' \quad (28)$$

Where $P_z(t) = \frac{1}{3} + \frac{2}{3}(1-\Delta^2 t^2)\exp\left(-\frac{1}{2}.\frac{t^2}{\tau_o^2}\right)$

Δ is the RMS width of the field distribution, $\tau_o$is the jump rate i.e. the residence time in each potential well. At resonance, the two jump rates equalize i.e. $t - t' = 0$, therefore at this point, $t = t'$.Equation (28) becomes

$$P(t) = P_z(t)\exp\left(-\frac{t}{\tau_o}\right) + \frac{1}{\tau_o}\int_0^t P_z(t)\exp\left(-\frac{t}{\tau_o}\right).P_z(0)dt \quad (29)$$

The result is thus

$$F(\Delta) = 2\pi\left(\frac{t+\Delta t^2}{8\tau_o}\right)\exp\left(\frac{-t^2-2t\tau_o+2i\omega\tau_o^2}{2\tau_o^2}\right) \quad (30)$$

Equating equation (30) to its equivalent in eqn. (8) gives the solutions

$$\frac{v_c}{v_{ab}} = \frac{\tau_o^2}{\Delta\omega^2} \quad (31)$$

or

$$\frac{v_{ab}}{v_c} = -2\pi\Delta\omega\left(\frac{t+\Delta t^2}{8\tau_o}\right)\exp\left(\frac{t^2 - 2t\tau_o+2i\omega\tau_o^2}{2\tau_o^2}\right) \quad (32)$$

An assumption was made at the low limit when $\exp\left(\frac{-t^2-2t\tau_o+2i\omega\tau_o^2}{2\tau_o^2}\right) \ll 1$, leaving the answers as

$$\frac{v_c}{v_{ab}} \cong -\frac{1}{2\pi\Delta\omega}\left(\frac{8\tau_o}{t+\Delta t^2}\right) \quad (33)$$

Barford (2009) showed that the measured effective penetration depth $\lambda_{\perp}$ is independent of the anisotropy ratio because it solely dependent on the in-plane penetration depth λ_{ab}

$$\lambda_{\perp} = f_{anisotropy} \cdot \lambda_{ab}$$

In furtherance with the investigation on the relational dependence of the anisotropy ratio and the phase angles (ωt) as shown in the Figure 5.

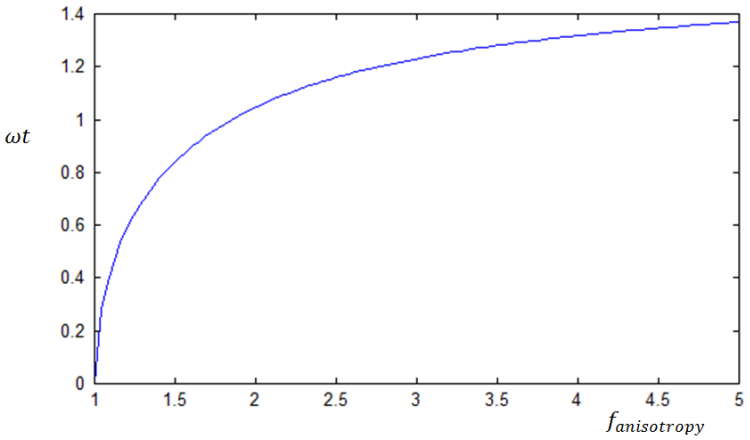

Figure 5: The effect of the phase angle on the anisotropic ratio

3.0 RESULTS AND DISCUSSION

The Gaussian events have been proven to initiate the computation of penetration length and vortex size of cylindrical HTS samples. The temperature dependence of the in-plane and out-plane penetration depth around T_c shown in homogeneous nanoscale superconducting domains was proven in Figure 2, Figure 3 and equation (27). Generally, the power law variation was observed which may signify the presence of nodes in the superconducting gap. Equation (27) reveals the possible effects of reversible magnetization $\frac{dM}{d\ln H}$ as discussed by Prozorov and Giannette (2006). The inter and intra band scattering which was believed to strongly affect the superconducting anisotropy of two-band superconductor (Kogan *et al.,* 2003) was visited in Figure 65. It was shown that, beyond the explanation of Kogan, the phase angle variation of the transverse magnetic field could also be a reason for the changes observed in the superconducting anisotropy of two-band superconductor and the temperature dependence of the anisotropy ratio in the inter-band scattering. At the superconducting state, the jump rate increases as temperature, beyond which, it has been established in equation (33) that an increase in the jump rates fosters an increase in the penetration velocity ratio. The same equation (33) reveals that the penetration velocity ratio decreases as the transverse magnetization increases as well as the root mean square of the field distribution. The penetration velocity can be extracted (like the penetration depth) from the traditional resonant circuit measurement technique with no additional devices. Figure 3 elaborates what happens at the mixed state (in between the first and second critical fields of the Meissner state). Different magnetic fields were analyzed within the mixed state. It was observed that though the magnitude of the superconducting state changes, its properties does not change. The penetration depth analysis under the changes of the phase angles (Figure 4) shows a Gaussian distribution which can be used to compute the penetration depths of other HTS shapes other cylindrical shapes.

4.0 CONCLUSION

At the superconducting state (under the muon spin relaxation rate), the jump rate increases as temperature, beyond which, it was establish that an increase in the jump rates fosters an increase in the penetration velocity ratio. Another way of measuring the magnetic penetration depth has been introduced-penetration velocity ratio which is subject to further investigation. The restriction of the Gaussian distribution to computing penetration depths of cylindrical HTS has been proven for other shapes of HTS.

ACKNOWLEDGMENTS

This work is self-funded. We appreciate Mrs. Jennifer Emetere for editing the script. We appreciate the Head of Physics Department of the above named institution.

REFERENCES

[1] Prozorov, R., Gannietta, R., Fournier, P. and Grenee, R. (2000): Magnetic Penetration Depth In Electron Doped Cuprates-Evidence In A Gap Node. *Physica C* 341-348, pp.1703-1704.

[2] Fumiaki Hayashi, Eiji Ueda, Masatoshi Sato, Kenji Kurahashi and Kazuyoshi Yamada (1998): Anisotropy Of The Superconducting Order Parameter Of $Nd_{2-x}Ce_xCuO_4$. *J.Phys. Soc. Japan*.67, pp.3234-3239.

[3] Gordon, R.T., Vannette, M.D., Martin, C., Nakajima, Y., Tamegai, T. and Prozorov, R. (2008): Two-Gap Superconductivity Seen In Penetration-Depth Measurements Of $Lu_2Fe_3Si_5$ Single Crystals Nodes. *Phy Rev B* 78, 024514.

[4] Awojoyogbe, O.B. (2003): A Mathematical Model Of Bloch NMR Equations For Quantitative Analysis Of Blood Flow In Blood Vessels With Changing Cross-Section II. *Physica A*, Vol. 323c, pp.534-550.

[5] Awojoyogbe O.B. (2004): Analytical Solution of the Time Dependent Bloch NMR Equations: A Translational Mechanical Approach' *Physica A*, Vol. 339, pp.437-460.

[6] Wigner, E.P. (1932): On The Quantum Correction For Thermodynamic Equilibrium. *Phys. Rev*. 40, pp.749–759

[7] Kirkwood, J.G (1993): Quantum Statistics Of Almost Classical Ensembles. *Phy Rev* 44, pp.31-37.

[8] O'Connell, R.F. and Lipo Wang (1985): Phase-Space Representations Of The Bloch Equation**.** *Phy Rev* 31, pp.1707-1711.

[9] Pattanaik, S.N. and Mudur, S.P. (1993): Computation Of Global Illumination In A Participating Medium By Monte Carlo Simulation. *The Journal of Visualisation and Computer Animation*. Vol. 4(3), pp.133-152.

[10] Hayano, R.S., Uemura, Y.J., Imazato, j., Nishida, N., Yamazaki, T. and Kubo R. (1979): Zero- And Low-Field Spin Relaxation Studied By Positive Muon. *Phys. Rev.* B20, pp.850-859.

[11] Bradford, R.A.W. (2009): Spatial Entanglement Of Formation In Thermal States Of One Or Two Identical Non-Interacting Massive Bosons. *International Journal of Theoretical Physics* vol. 48, No. 8, pp.2328-2339.

[12] Prozorov, R. and Giannetta, R.W. (2006): Magnetic Penetration Depth In Unconventional Superconductors. *supercond. Sci. technol*. 19, pp.41-67

[13] Kogan, A., Granger, G., Kastner, M.A. and Goldhaber-Gordon D. (2003): Singlet–Triplet Transition In A Single-Electron Transistor At Zero Magnetic Field. *Physical Review B* 67, 113309 pp.1-4.